Research Article

Nauman Ahmed, Jorge E. Macías-Díaz*, Makhdoom Ali, Muhammad Jawaz, Muhammad Z. Baber, and María G. Medina-Guevara

Dynamical wave structures for some diffusion–reaction equations with quadratic and quartic nonlinearities

https://doi.org/10.1515/phys-2024-0115
received October 03, 2024; accepted January 08, 2025

Abstract: This work investigates the quadratic and quartic nonlinear diffusion–reaction equations with nonlinear convective flux terms, which are investigated analytically. Diffusion–reaction equations have a wide range of applications in several scientific areas, such as chemistry, biology, and population dynamics of the species. The new extended direct algebraic method is applied to obtain abundant families of solitary wave solutions. Different types of solitary wave solutions are obtained by applying this analytical method. This approach provides the solutions in the form of single and combined wave structures, which are observed in shock, complex solitary-shock, shock-singular, and periodic-singular forms. Some of the solutions are depicted graphically to illustrate the fact that they are, indeed, wave solutions of the mathematical model.

Keywords: extended direct algebraic method, quadratic and quartic nonlinearities, soliton solutions, traveling-wave solutions

*** Corresponding author: Jorge E. Macías-Díaz,** Department of Mathematics and Didactics of Mathematics, School of Digital Technologies, Tallinn University, Tallinn, Estonia; Departamento de Matemáticas y Física, Universidad Autónoma de Aguascalientes, Aguascalientes, Mexico, e-mail: jorge.macias_diaz@tlu.ee, jorge-maciasdiaz@edu.uaa.mx, jemacias@correo.uaa.mx
Nauman Ahmed: Department of Mathematics and Statistics, The University of Lahore, Lahore, Pakistan; Department of Computer Science and Mathematics, Lebanese American University, Beirut, Lebanon, e-mail: nauman.ahmed@math.uol.edu.pk
Makhdoom Ali: Department of Mathematics and Statistics, The University of Lahore, Lahore, Pakistan, e-mail: alimakhdoom14@gmail.com
Muhammad Jawaz: Department of Mathematics and Statistics, The University of Lahore, Lahore, Pakistan, e-mail: zafarullah8883@gmail.com
Muhammad Z. Baber: Department of Mathematics and Statistics, The University of Lahore, Lahore, Pakistan, e-mail: muhammad.jawaz@math.uol.edu.pk
María G. Medina-Guevara: Department of Exact Sciences and Technology, Los Lagos University Center, University of Guadalajara, Jalisco, Mexico, e-mail: mguadalupe.medina@lagos.udg.mx

1 Introduction

In the physical sciences, differential equations (DEs) are essential to describe some physical phenomena. Many important evolutionary occurrences are often modeled by nonlinear partial differential equations (NPDEs). Most physical phenomena in various fields, such as field theory, optical fiber [1,2], mathematical physics, plasma physics [3], biophysics, fluid dynamics, mechanics, aerospace industry [4], chemistry reactions [5–7], metrology, and many other fields [8–10] are described by using the NPDEs. For instance, the nonlinear Schrödinger equation (NLSE) has numerous applications in scientific fields such as nonlinear optics, mathematical finance, plasma physics, nuclear and solid-state physics, biochemistry, superconductivity, and matter.

As most of the physical occurrences are modeled by NPDEs. It is essential to find the solutions to NPDEs. Finding the solutions to the NPDEs is crucial to having a thorough understanding of the phenomenon. To obtain the exact solution, a range of analytical techniques have been developed and reported in the literature. The Kudryashov method [11], the homogenous balance method [12,13], the generalized Kudryashov method [14,15], the tanh–coth method [16,17], the direct algebraic method, extended modified auxiliary equation mapping method, the unified method, the modified and extended rational expansion method, the extended $(\frac{G'}{G})$-expansion technique, the variational principle method [18,19], the amplitude ansatz method [20], the bilinear neural network method [21], the auxiliary equation method [22], the improved P-expansion approach [23], the improved modified extended tanh-function method [24], the generalized algebraic method, the Jacobian elliptic functions technique [25], the

improved $\exp(-F(\eta))$-expansion method [26], the Riccati equation method [27], the modified $(\frac{G'}{G})$-expansion method [28] among others, have been developed to this end.

It is worth pointing out that Yan and Lou worked on the soliton molecules of Sharma–Tasso–Olver–Burgers equation [29], Wu *et al.* investigated the nonlinear von Karman equations for the three-layer microplates [30]. Meanwhile, Wang *et al.* considered the diffusively delay-coupled memristive Chialvo neuron map for the network patterns [31], while Dai *et al.* worked on the macrodispersivity models with an analytical solution [32]. Kai and Yin worked on the Gaussian traveling wave solution to a special kind of Schrödinger equation [33], Zhu *et al.* used the logarithmic transformation for the modified Schrödinger's equation [34] and nonlinear Zakharov system [35] to obtain analytical solutions. Berkal and Almatrafi worked on the bifurcation and stability of a two-dimensional activator–inhibitor model [36], and some researchers have worked on the approximate solutions of reaction–diffusion models [37–40]. in the present study, we will derive exact solutions for a nonlinear reaction–diffusion system.

Our current research focuses on nonlinear diffusion–reaction (DR) equations, which have wide applications in biology, chemical, physical, and logical systems. Various reduced versions of the DR equations have been investigated in the literature. In the study by Triki *et al.* [41], the auxiliary equation method was used to study three nonlinear DR equations in inhomogeneous mediums, including derivative-type and algebraic-type nonlinearities. Furthermore, nonlinear reaction diffusion equations with cubic and quantic nonlinearities, nonlinear DR equations including quadratic-cubic nonlinearities, and nonlinear diffusion–reaction equations with a nonlinear convective flux term have been investigated by Bhardwaj *et al.* [42], Malik *et al.* [43,44]. We examine the DR equation for a case where the diffusion coefficient D is unaffected by density.

In the present work, we investigate the dynamics through the solutions of particular nonlinear DR equations, which include a nonlinear convective flux term along with quadratic and biquadratic nonlinearities and are represented by the following equations:

$$\varphi_t + k\varphi\varphi_x = D\varphi_{xx} + \alpha\varphi - \beta\varphi^2, \tag{1}$$

$$\varphi_t + k\varphi^2\varphi_x = D\varphi_{xx} + \alpha\varphi - \beta\varphi^4, \tag{2}$$

where α, β, and k are physical constants that need to be determined, D is the diffusion coefficient, and $\varphi = \varphi(x, t)$ has different interpretations according to the phenomenon under investigation. These equations describe transport phenomena where diffusion and convection processes are equally important and nonlinear diffusion is assumed to be similar to nonlinear convection effects. The $(\frac{G'}{G})$-expansion method and the Kudryashov method have been recently applied to solve this system of equations.

The purpose of this study is to improve the accuracy of possible soliton solutions of the DR equations through a new methodology. Being a novel analytical technique, the new extended direct algebraic method (NEDAM) has not been applied to solve nonlinear DR equations with a nonlinear convective flux term. In domains including engineering, physics, and applied mathematics, NEDAM has demonstrated its reliability and effectiveness in resolving NPDEs. For example, Vahidi [45], Mirhosseini-Alizamini *et al.* [46], and Munawar *et al.* [47] have used NEDAM to solve different types of NPDEs. Furthermore, Kurt *et al.* used NEDAM to find traveling and solitary wave solutions of the potential Kadomtsev–Petviashvili equation. The author found that the NEDAM is accurate, effective, and applicable for solving problems. There are many other methods that provided us with hyperbolic, trigonometric, and rational function solutions. As we will see, single and combined wave structures are observed in shock, complex solitary-shock, shock-singular, and periodic-singular forms. Rational solutions also emerged during the derivation.

The present work is organized as follows. Section 2 is devoted to provide a brief summary of the NEDAM. To that end, we employ [48] as a guiding reference. The methodology is explained in its most general setting. We provide therein a set of steps that lead to the derivation of exact traveling-wave solutions of general systems of partial DEs in two variables, namely, space and time. Moreover, various cases are fully described to reach exact solutions for those models. In turn, Section 3 is devoted to derive the exact traveling-wave solutions for the mathematical models (1) and (2). From our discussion, it can be readily checked the existence of abundant solutions of this form for our mathematical models. For the sake of convenience, we illustrate the behavior of just some of those solutions by means of three-dimensional plots, contour plots, and two-dimensional plots. As we can see from the figures, all of the solutions obtained through the NEDAM are traveling waves. Finally, we close this work with a section of concluding remarks.

2 Method

In this section, we provide an outline of the NEDAM [48]. This method consists of the next steps.

Step 1. We suppose that a NLPDE can be expressed as follows:

$$H(M, M_t, M_x, M_{tt}, M_{xt}, M_{xx}, \ldots) = 0, \tag{3}$$

where M is an unknown function and H is a polynomial of $M(x, t)$.

Step 2. Consider the transformation $M(x, t) = \psi(\zeta)$, where $\zeta = x - wt$. Here, w indicates the wave velocity. By substituting this transformation into (3), we obtain

$$\psi(\varphi, \varphi', \varphi'', \varphi''', \ldots) = 0, \tag{4}$$

where $\varphi = \varphi(\zeta)$, $\varphi' = \frac{d\varphi}{d\zeta}$, $\varphi'' = \frac{d^2\varphi}{d\zeta^2}$, etc.

Step 3. We assume that (4) has a solution of the form

$$\varphi(\zeta) = \sum_{i=0}^{N} b_i \Omega^i(\zeta), \tag{5}$$

where $b_i (0 \le i \le N)$ are unknown constants, $b_N \neq 0$, and $\Omega(\zeta)$ satisfies the auxiliary ordinary differential equation (ODE):

$$\Omega'(\zeta) = \ln F(m + n\Omega(\zeta) + v\Omega(\zeta)^2), \quad F \neq 0, 1, \tag{6}$$

where m, n, and v are constants. The solution to Eq. (6) can be expressed as follows:

- If $n^2 - 4mv < 0$ and $v \neq 0$, then we have

$$\Omega_1(\zeta) = -\frac{n}{2v} + \Phi_1 \tan_F\left(\frac{\sqrt{-(n^2 - 4mv)}}{2}\zeta\right), \tag{7}$$

$$\Omega_2(\zeta) = -\frac{n}{2v} + \Phi_1 \cot_F\left(\frac{\sqrt{-(n^2 - 4mv)}}{2}\zeta\right), \tag{8}$$

$$\Omega_3(\zeta) = -\frac{n}{2v} + \Phi_1 \tan_F(\sqrt{-(n^2 - 4mv)}) \pm \sqrt{pq}\, \sec_F(\sqrt{-n^2 - 4mv}\,\zeta), \tag{9}$$

$$\Omega_4(\zeta) = -\frac{n}{2v} + \Phi_1 \cot_F(\sqrt{-(n^2 - 4mv)}) \pm \sqrt{pq}\, \csc_F(\sqrt{-n^2 - 4mv}\,\zeta), \tag{10}$$

$$\Omega_5(\zeta) = -\frac{n}{2v} + \frac{\Phi_1}{2}\tan_F\left(\frac{\sqrt{-(n^2 - 4mv)}}{4}\right) - \cot_F\left(\frac{\sqrt{-n^2 - 4mv}}{4}\zeta\right), \tag{11}$$

where

$$\Phi_1 = \frac{\sqrt{-(n^2 - 4mv)}}{2v}. \tag{12}$$

- If $n^2 - 4mv > 0$ and $v \neq 0$, then

$$\Omega_6(\zeta) = -\frac{n}{2v} - \Phi_2 \tanh_F\left(\frac{\sqrt{n^2 - 4mv}}{2}\zeta\right), \tag{13}$$

$$\Omega_7(\zeta) = -\frac{n}{2v} - \Phi_2 \coth_F\left(\frac{\sqrt{n^2 - 4mv}}{2}\zeta\right), \tag{14}$$

$$\Omega_8(\zeta) = -\frac{n}{2v} - \Phi_2 \tanh_F(\sqrt{n^2 - 4mv}) \pm \iota\sqrt{pq}\, \mathrm{sech}_F(\sqrt{n^2 - 4mv}\,\zeta), \tag{15}$$

$$\Omega_9(\zeta) = -\frac{n}{2v} - \Phi_1 \coth_F(\sqrt{-(n^2 - 4mv)}) \pm \sqrt{pq}\, \mathrm{csch}_F(\sqrt{n^2 - 4mv}\,\zeta), \tag{16}$$

$$\Omega_{10}(\zeta) = -\frac{n}{2v} + \frac{\Phi_1}{2}\left(\tanh_F\left(\frac{\sqrt{-(n^2 - 4mv)}}{4}\right) - \coth_F\left(\frac{\sqrt{-n^2 - 4mv}}{4}\zeta\right)\right), \tag{17}$$

where

$$\Phi_2 = \frac{\sqrt{n^2 - 4mv}}{2v}. \tag{18}$$

- If $mv > 0$ and $n = 0$, then

$$\Omega_{11}(\zeta) = \sqrt{\frac{m}{v}}\, \tan_F(\sqrt{mv}\,\zeta), \tag{19}$$

$$\Omega_{12}(\zeta) = -\sqrt{\frac{m}{v}}\, \cot_F(\sqrt{mv}\,\zeta), \tag{20}$$

$$\Omega_{13}(\zeta) = \sqrt{\frac{m}{v}}\,(\tan_F(2\sqrt{mv}\,\zeta) \pm \sqrt{pq}\, \sec_F(2\sqrt{mv}\,\zeta)), \tag{21}$$

$$\Omega_{14}(\zeta) = \sqrt{\frac{m}{v}}\,(-\cot_F(2\sqrt{mv}\,\zeta) \pm \sqrt{pq}\, \csc_F(2\sqrt{mv}\,\zeta)), \tag{22}$$

$$\Omega_{15}(\zeta) = \frac{1}{2}\sqrt{\frac{m}{v}}\left(\tan_F\left(\frac{\sqrt{mv}}{2}\zeta\right) - \cot_F\left(\frac{\sqrt{mv}}{2}\zeta\right)\right). \tag{23}$$

- If $mv < 0$ and $n = 0$, then

$$\Omega_{16}(\zeta) = -\sqrt{-\frac{m}{v}}\, \tanh_F(\sqrt{-mv}\,\zeta), \tag{24}$$

$$\Omega_{17}(\zeta) = -\sqrt{-\frac{m}{v}}\, \coth_F(\sqrt{-mv}\,\zeta), \tag{25}$$

$$\Omega_{18}(\zeta) = \sqrt{-\frac{m}{v}}\,(-\tanh_F(2\sqrt{-mv}\,\zeta) \pm \iota\sqrt{mv}\, \mathrm{sech}_F(2\sqrt{-mv})), \tag{26}$$

$$\Omega_{20}(\zeta) = -\frac{1}{2}\sqrt{-\frac{m}{v}}\left(\tan_F\left(\frac{\sqrt{-mv}}{2}\zeta\right) + \cot_F\left(\frac{\sqrt{-mv}}{2}\zeta\right)\right). \tag{27}$$

- If $n = 0$ and $v = m$, then

$$\Omega_{21}(\zeta) = \tan_F(m\zeta), \tag{28}$$

$$\Omega_{22}(\zeta) = -\cot_F(m\zeta), \tag{29}$$

$$\Omega_{23}(\zeta) = \tan_F(2m\zeta) \pm \sqrt{pq}\sec_F(2m\xi), \tag{30}$$

$$\Omega_{24}(\zeta) = -\cot_F(2m\zeta) \pm \sqrt{pq}\csc_F(2m\zeta), \tag{31}$$

$$\Omega_{25}(\zeta) = \frac{1}{2}\left(\tan_F\left(\frac{m}{2}\zeta\right) - \cot_F\left(\frac{m}{2}\zeta\right)\right). \tag{32}$$

- If $n = 0$ and $\nu = -m$, then

$$\Omega_{26}(\zeta) = -\tan_F(m\zeta), \tag{33}$$

$$\Omega_{27}(\zeta) = -\cot_F(m\zeta), \tag{34}$$

$$\Omega_{28}(\zeta) = -\tanh_F(2m\zeta) \pm \iota\sqrt{pq}\sec_F(2m\zeta), \tag{35}$$

$$\Omega_{29}(\zeta) = -\coth_F(2m\zeta) \pm \sqrt{pq}\,\mathrm{csch}_F(2m\zeta), \tag{36}$$

$$\Omega_{30}(\zeta) = -\frac{1}{2}\left(\tanh_F\left(\frac{m}{2}\zeta\right) + \coth_F\left(\frac{m}{2}\zeta\right)\right). \tag{37}$$

- If $n^2 = 4m\nu$, then

$$\Omega_{31}(\zeta) = \frac{-2m(n\zeta \ln F + 2)}{n^2\zeta \ln F}. \tag{38}$$

- If $n = \chi$, $m = r\chi$ with $(r \neq 0)$, and $\nu = 0$, then $\Omega_{32}(\zeta) = F^{\chi\zeta} - r$.
- If $n = \nu = 0$, then $\Omega_{33}(\xi) = \mu\xi \ln F$.
- If $n = m = 0$, then

$$\Omega_{34}(\zeta) = \frac{-1}{\nu\zeta \ln F}. \tag{39}$$

- If $=m = 0$ and $\nu \neq 0$, then

$$\Omega_{35}(\zeta) = -\frac{pn}{\nu(\cosh_F(n\zeta) - \sinh_F(n\zeta) + p)}, \tag{40}$$

$$\Omega_{36}(\zeta) = -\frac{n(\sinh_F(n\zeta) + \mathrm{c}osh_F(n\zeta))}{\nu(\sinh_F(n\zeta) + \cosh_F(n\zeta) + q)}. \tag{41}$$

- If $n = \chi$, $\nu = r\chi(r \neq 0)$ and $m = 0$, then

$$\Omega_{37}(\zeta) = \frac{pF^{\chi\zeta}}{p - rqI^{\chi\zeta}}. \tag{42}$$

It is worth recalling that the generalized hyperbolic and triangular functions are defined as follows:

$$\sinh_F(\zeta) = \frac{pF^{\zeta} - qF^{-\zeta}}{2}, \quad \cosh_F(\zeta) = \frac{pF^{\zeta} + qF^{-\zeta}}{2}, \tag{43}$$

$$\tanh_F(\zeta) = \frac{pF^{\zeta} - qF^{-\zeta}}{pF^{\zeta} + qF^{-\zeta}}, \quad \coth_F(\zeta) = \frac{pF^{\zeta} + qF^{-\zeta}}{pF^{\zeta} - qF^{-\zeta}}, \tag{44}$$

$$\mathrm{sech}_F(\zeta) = \frac{2}{pF^{\zeta} + qF^{-\zeta}}, \quad \mathrm{csch}_F(\zeta) = \frac{2}{pF^{\zeta} - qF^{-\zeta}}, \tag{45}$$

$$\sin_F(\zeta) = \frac{pF^{\iota\zeta} - qF^{-\iota\zeta}}{2}, \quad \cos_F(\zeta) = \frac{pF^{\iota\zeta} + qF^{-\iota\zeta}}{2}, \tag{46}$$

$$\tan_F(\zeta) = -\iota\frac{pF^{\zeta} - qF^{-\iota\zeta}}{pF^{\zeta} + qF^{-\iota\zeta}}, \quad \cot_F(\zeta) = -\iota\frac{pF^{\zeta} + qF^{-\iota\zeta}}{pF^{\zeta} - qF^{-\iota\zeta}}, \tag{47}$$

$$\sec_F(\zeta) = \frac{2}{pF^{\iota\zeta} + qF^{-\iota\zeta}}, \quad \csc_F(\zeta) = \frac{2\iota}{pF^{\iota\zeta} - qF^{-\iota\zeta}}, \tag{48}$$

where ζ is an independent variable and $p, q > 0$.

Step 4. Calculate N using the balancing method on Eq. (4).

Step 5. Combine Eq. (5) together with Eq. (4), set coefficients of $\Omega(\zeta)$ equal to zero, and determine the values of the unknowns.

3 Results

The present section is divided into two stages. In Section 3.1, we derive exact solutions for the quadratic model and, Section 3.2, we obtain solutions for the quartic model.

3.1 Quadratic model

To obtain soliton solutions of the DR equations under study in the present work, we employ the traveling-wave transformation $\zeta = x - wt$, so that $\varphi(x, t) = \psi(\zeta)$. This change of variable transforms Eqs. (1) and (2) into the following nonlinear ODE:

$$D\psi'' + w\psi' - k\psi^2\psi' + \alpha\psi - \beta\psi^2 = 0, \tag{49}$$

where the prime symbol denotes the order of derivative of the function ψ with respect to ζ. By applying the homogeneous balancing criterion to Eq. (49), one can readily find that $N = 1$. Therefore, we can write the solutions of Eq. (49) as follows:

$$\psi(\zeta) = b_0 + b_1\Omega(\zeta). \tag{50}$$

By using Eq. (50) and its derivative in Eq. (49) and by equating the coefficient of the powers of $\Omega(\zeta)$ zero, one can obtain a system of algebraic equations. It is easy to check that the solution of this system of equations is given by

$$b_0 = \frac{Dkn\log F - \sqrt{D^2k^2n^2\log^2 F - 4D^2k^2m\nu\log^2 F}}{k^2}, \tag{51}$$

$$b_1 = \frac{2D\nu\log F}{k}, \tag{52}$$

$$w = \frac{2D\beta - \sqrt{D^2k^2\log^2 F(n^2 - 4m\nu)}}{k}, \tag{53}$$

$$\alpha = -\frac{2\beta\sqrt{D^2k^2\log^2 F(n^2 - 4m\nu)}}{k^2}. \tag{54}$$

By manipulating Eq. (50) along with the different forms of $\Omega(\zeta)$ described in Section 2, we can obtain the following forms of traveling wave solutions for Eq. (1):

- When $n^2 - 4mv < 0$ and $v \neq 0$, then

$$\varphi_1(x,t) = \frac{1}{k^2}(Dkn\ln F - D\sqrt{\sigma}k\ln(F)) + \frac{1}{k}\left\{2Dv\ln(F)\left(\frac{\sqrt{-\alpha}\tan_F\left(\frac{\zeta\sqrt{-\sigma}}{2}\right)}{2v} - \frac{n}{2v}\right)\right\}, \quad (55)$$

$$\varphi_2(x,t) = \frac{1}{k^2}(Dkn\ln(F) - Dk\sqrt{\sigma}\ln(F)) + \frac{1}{k}\left\{2Dv\ln(F)\left(-\frac{\sqrt{-\sigma}\cot_F\left(\frac{\zeta\sqrt{-\sigma}}{2}\right)}{2v} - \frac{n}{2v}\right)\right\}, \quad (56)$$

$$\varphi_3(x,t) = \frac{1}{k^2}(Dkn\ln(F) - Dk\sqrt{\sigma}\ln(F)) + \frac{1}{k}\left\{2Dv\ln(F)\left(\frac{\sqrt{-\sigma}(\tan_F(\zeta\sqrt{-\sigma}) - \sec_F(\zeta\sqrt{-\sigma}))}{2v} - \frac{n}{2v}\right)\right\}, \quad (57)$$

$$\varphi_4(x,t) = \frac{1}{k^2}(Dkn\ln(F) - Dk\sqrt{\sigma}\ln(F)) + \frac{1}{k}\left\{2Dv\ln(F)\left(-\frac{\sqrt{\sigma}(\cot_F(\zeta\sqrt{-\sigma}) - \csc_F(\zeta\sqrt{-\sigma}))}{2v} - \frac{n}{2v}\right)\right\}, \quad (58)$$

$$\varphi_5(x,t) = \frac{1}{k^2}(Dkn\ln(F) - Dk\sqrt{\sigma}\ln(F)) + \frac{1}{k}\left\{2Dv\ln(F)\left(\frac{\sqrt{-\sigma}\left(\tan_F\left(\frac{\zeta\sqrt{-\sigma}}{4}\right) - \cot_F\left(\frac{\zeta\sqrt{-\sigma}}{4}\right)\right)}{4v} - \frac{n}{2v}\right)\right\}, \quad (59)$$

where $\sigma = n^2 - 4mv$. For illustration purposes, Figure 1 behavior of the solution $\varphi_1(x,t)$ for the parameter values $n = 1.5$, $m = 1.5$, $v = 1.5$, $\beta = 1.9$, $k = 1.4$, $F = 1.5$, and $D = 1.4$.

- When $n^2 - 4mv > 0$ and $v \neq 0$, then

$$\varphi_6(x,t) = \frac{1}{k^2}(Dkn\ln(F) - Dk\sqrt{\sigma}\ln(F)) + \frac{1}{k}\left\{2Dv\ln(F)\left(-\frac{n}{2v} - \frac{\sqrt{\sigma}\tanh_F\left(\frac{\zeta\sqrt{\sigma}}{2}\right)}{2v}\right)\right\}, \quad (60)$$

$$\varphi_7(x,t) = \frac{1}{k^2}(Dkn\ln(F) - Dk\sqrt{\sigma}\ln(F)) + \frac{1}{k}\left\{2Dv\ln(F)\left(-\frac{\sqrt{\sigma}\coth_F\left(\frac{\zeta\sqrt{\sigma}}{2}\right)}{2v} - \frac{n}{2v}\right)\right\}, \quad (61)$$

$$\varphi_8(x,t) = \frac{1}{k^2}(Dkn\ln(F) - Dk\sqrt{\sigma}\ln(F)) + \frac{1}{k}\left\{2Dv\ln(F)\left(-\frac{n}{2v} - \frac{\sqrt{\sigma}(\tanh_F(\zeta\sqrt{\sigma}) - i\operatorname{sech}_F(\zeta\sqrt{\sigma}))}{2v}\right)\right\}, \quad (62)$$

$$\varphi_9(x,t) = \frac{1}{k^2}(Dkn\ln(F) - D\sqrt{\sigma}k\ln(F)) + \frac{1}{k}\left\{2Dv\ln(F)\left(-\frac{\sqrt{\sigma}(\coth_F(\zeta\sqrt{\sigma}) - \operatorname{csch}_F(\zeta\sqrt{\sigma}))}{2v} - \frac{n}{2v}\right)\right\}, \quad (63)$$

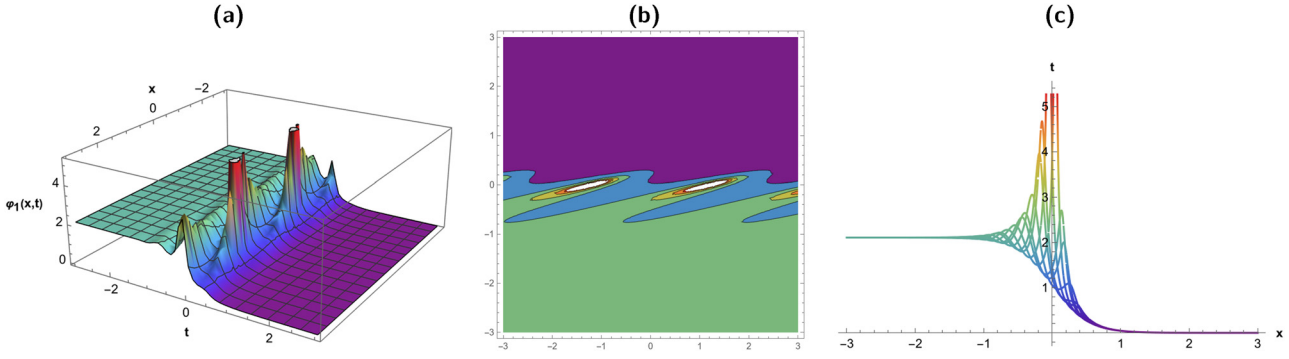

Figure 1: Lump-kink soliton behavior of the solution $\varphi_1(x,t)$ for the parameter values $n = 1.5$, $m = 1.5$, $v = 1.5$, $\beta = 1.9$, $k = 1.4$, $F = 1.5$, and $D = 1.4$: (a) three-dimensional plot, (b) contour plot, and (c) two-dimensional plot.

$$\varphi_{10}(x,t)=\frac{1}{k^2}(Dkn\ln(F)-D\sqrt{\sigma}k\ln(F))+\frac{1}{k}\left\{2Dv\ln(F)\left(-\frac{\sqrt{\sigma}\left(\coth_F\left(\frac{\zeta\sqrt{\sigma}}{4}\right)+\tanh_F\left(\frac{\zeta\sqrt{\sigma}}{4}\right)\right)}{4v}-\frac{n}{2v}\right)\right\}. \tag{64}$$

Figure 2 shows the graphical behavior of the solution $\varphi_6(x,t)$ for the parameter values $n=0.1$, $m=-1$, $v=0.2$, $\beta=1.2$, $k=0.1$, $F=1.5$, and $D=1.1$.

- If $mv>0$ and $n=0$, then

$$\varphi_{11}(x,t)=\frac{1}{k^2}(Dkn\ln(F)-Dk\sqrt{\sigma}\ln(F))+\frac{1}{k}\left\{2Dv\ln(F)\sqrt{\frac{m}{v}}\tan_F(\zeta\sqrt{mv})\right\}, \tag{65}$$

$$\varphi_{12}(x,t)=\frac{1}{k^2}(Dkn\ln(F)-Dk\sqrt{\sigma}\ln(F))-\frac{1}{k}\left\{2Dv\ln(F)\sqrt{\frac{m}{v}}\cot_F(\zeta\sqrt{mv})\right\}, \tag{66}$$

$$\varphi_{13}(x,t)=\frac{1}{k^2}(Dkn\ln(F)-Dk\sqrt{\sigma}\ln(F))+\frac{1}{k}\left\{2Dv\ln(F)\left(\sqrt{\frac{m}{v}}\tan_F(2\zeta\sqrt{mv})-\sqrt{pq}\sec_F(2\zeta\sqrt{mv})\right)\right\}, \tag{67}$$

$$\varphi_{14}(x,t)=\frac{1}{k^2}(Dkn\ln(F)-Dk\sqrt{\sigma}\ln(F))+\frac{1}{k}\left\{2Dv\ln(F)\left(\sqrt{pq}\csc_F(2\zeta\sqrt{mv})-\sqrt{\frac{m}{v}}\cot_F(2\zeta\sqrt{mv})\right)\right\}, \tag{68}$$

$$\varphi_{15}(x,t)=\frac{1}{k^2}(Dkn\ln(F)-Dk\sqrt{\sigma}\ln(F))+\frac{1}{k}\left\{Dv\ln(F)\sqrt{\frac{m}{v}}\left(\tan_F\left(\frac{1}{2}\zeta\sqrt{mv}\right)-\cot_F\left(\frac{1}{2}\zeta\sqrt{mv}\right)\right)\right\}. \tag{69}$$

Figure 3 shows the graphical behavior of the solution $\varphi_{11}(x,t)$ for the parameter values $n=0$, $m=0.1$, $v=1.5$, $\beta=0.4$, $k=0.2$, $F=1.2$, and $D=2$.

- If $mv<0$ and $n=0$, then

$$\varphi_{16}(x,t)=\frac{1}{k^2}(Dkn\ln(F)-D\sqrt{\sigma}k\ln(F))-\frac{1}{k}\left\{2Dv\ln(F)\sqrt{-\frac{m}{v}}\tanh_F(\zeta\sqrt{-mv})\right\}, \tag{70}$$

$$\varphi_{17}(x,t)=\frac{1}{k^2}(Dkn\ln(F)-Dk\sqrt{\sigma}\ln(F))-\frac{1}{k}\left\{2Dv\ln(F)\sqrt{-\frac{m}{v}}\coth_F(\zeta\sqrt{-mv})\right\}, \tag{71}$$

$$\varphi_{18}(x,t)=\frac{1}{k^2}(Dkn\log F-Dk\sqrt{\sigma}\ln(F))-\frac{1}{k}\left\{2Dv\ln(F)\sqrt{-\frac{m}{v}}(\tanh_F(2\zeta\sqrt{-mv})+i\sqrt{pq}\,\mathrm{sech}_F(2\zeta\sqrt{-mv}))\right\}, \tag{72}$$

$$\varphi_{19}(x,t)=\frac{1}{k^2}(Dkn\ln(F)-D\sqrt{\sigma}kLn(F))-\frac{1}{k}\left\{2Dv\ln(F)\sqrt{-\frac{m}{v}}(\sqrt{pq}\coth_F(2\sqrt{-mv})+\mathrm{csch}_F(2\sqrt{-mv}))\right\}, \tag{73}$$

$$\varphi_{20}(x,t)=\frac{1}{k^2}(Dkn\ln(F)-D\sqrt{\sigma}k\ln(F))-\frac{1}{k}\left\{Dv\ln(F)\sqrt{-\frac{m}{v}}\left(\tanh_F\left(\frac{1}{2}\zeta\sqrt{-mv}\right)-\coth_F\left(\frac{1}{2}\zeta\sqrt{-mv}\right)\right)\right\}. \tag{74}$$

For illustration purposes, Figure 4 shows the graphical behavior of the solution $\varphi_{16}(x,t)$ for the parameter values $n=0$, $m=-1$, $v=1.5$, $\beta=0.5$, $k=0.2$, $F=1.5$, and $D=1$.

- When $n=0$ and $m=v$, then

$$\varphi_{21}(x,t)=\frac{1}{k^2}(Dkn\ln(F)-D\sqrt{\sigma}k\ln(F))+\frac{1}{k}(2Dv\ln(F)\tan_F(\zeta m)), \tag{75}$$

$$\varphi_{22}(x,t)=\frac{1}{k^2}(Dkn\ln(F)-Dk\sqrt{\sigma}\ln(F))-\frac{1}{k}(2Dv\ln(F)\cot_F(\zeta m)), \tag{76}$$

$$\varphi_{23}(x,t)=\frac{1}{k^2}(Dkn\ln(F)-Dk\sqrt{\sigma}\ln(F))+\frac{1}{k}\{2\mathrm{D}v\ln(F)(\sec_F(2\zeta m)+\tan_F(2\zeta m))\}, \tag{77}$$

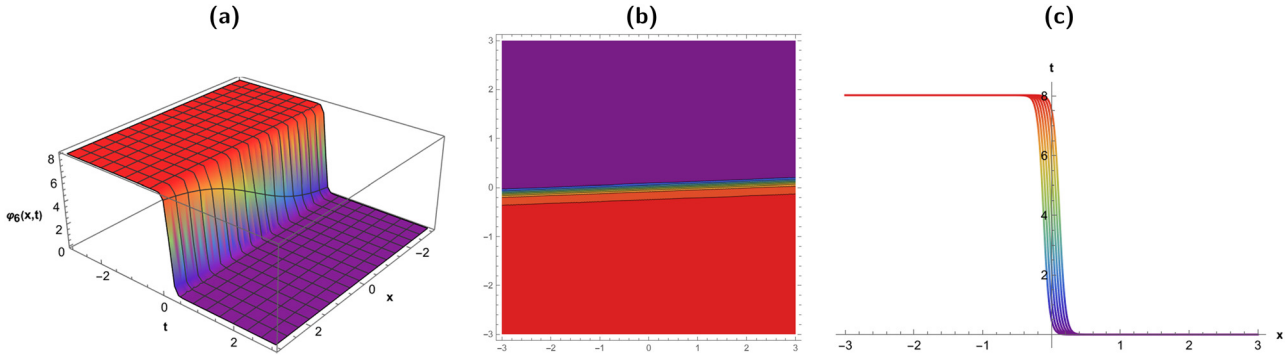

Figure 2: Kink soliton behavior of the solution $\varphi_6(x, t)$ for the parameter values $n = 0.1$, $m = -1$, $\nu = 0.2$, $\beta = 1.2$, $k = 0.1$, $F = 1.5$, and $D = 1.1$: (a) three-dimensional plot, (b) contour plot, and (c) two-dimensional plot.

$$\varphi_{24}(x,t) = \frac{1}{k^2}(Dkn\ln(F) - Dk\sqrt{\sigma}\ln(F)) + \frac{1}{k}\{2D\nu\ln(F)(\csc_F(2\zeta m) - \cot_F(2\zeta m))\}, \tag{78}$$

$$\varphi_{25}(x,t) = \frac{1}{k^2}(Dkn\ln(F) - Dk\sqrt{\sigma}\ln(F)) + \frac{1}{k}\left\{D\nu\ln(F)\left(\tan_F\left(\frac{\zeta m}{2}\right) - \cot_F\left(\frac{\zeta m}{2}\right)\right)\right\}. \tag{79}$$

- When $n = 0$ and $m = -\nu$, then

$$\varphi_{26}(x,t) = \frac{1}{k^2}(Dkn\ln(F) - D\sqrt{\sigma}k\ln(F)) - \frac{1}{k}(2D\nu\ln(F)\tanh_F(\zeta m)), \tag{80}$$

$$\varphi_{27}(x,t) = \frac{1}{k^2}(Dkn\ln(F) - Dk\sqrt{\sigma}\ln(F)) - \frac{1}{k}(2D\nu\ln(F)\coth_F(\zeta m)), \tag{81}$$

$$\varphi_{28}(x,t) = \frac{1}{k^2}(Dkn\ln(F) - \sqrt{\sigma}Dk\ln(F)) + \frac{1}{k}\{2\mathrm{D}\nu\ln(F)(-\tanh_F(2\zeta m) + i\sqrt{pq}\,\mathrm{sech}_F(2\zeta m))\}, \tag{82}$$

$$\varphi_{29}(x,t) = \frac{1}{k^2}(Dkn\ln(F) - Dk\sqrt{\sigma}\ln(F)) + \frac{1}{k}\{2D\nu\ln(F)(-\coth_F(2\zeta m) + i\sqrt{pq}\,\mathrm{csch}_F(2\zeta m))\}, \tag{83}$$

$$\varphi_{30}(x,t) = \frac{1}{k^2}(Dkn\ln(F) - Dk\sqrt{\sigma}\ln(F)) + \frac{1}{k}\left\{D\nu\ln(F)\left(-\coth_F\left(\frac{\zeta m}{2}\right) - \tanh_F\left(\frac{\zeta m}{2}\right)\right)\right\}. \tag{84}$$

- When $n^2 = 4m\nu$, then

$$\varphi_{31}(x,t) = \frac{1}{k^2}(Dkn\ln(F) - Dk\sqrt{\sigma}\ln(F)) - \frac{1}{\zeta kn^2}\{4Dm\nu(\zeta n\ln(F) + 2)\}. \tag{85}$$

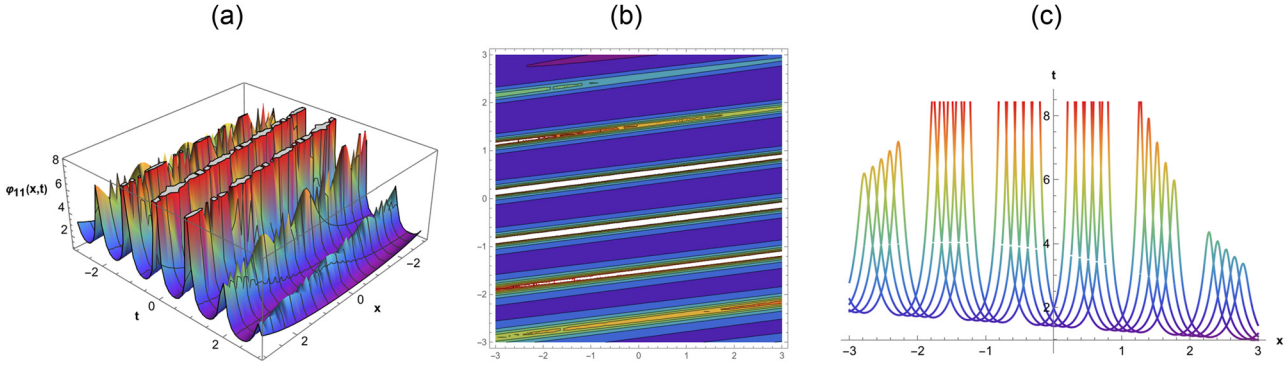

Figure 3: Solitary wave behavior of the solution $\varphi_{11}(x, t)$ for the parameter values $n = 0$, $m = 0.1$, $\nu = 1.5$, $\beta = 0.4$, $k = 0.2$, $F = 1.2$, and $D = 2$: (a) three-dimensional plot, (b) contour plot, and (c) two-dimensional plot.

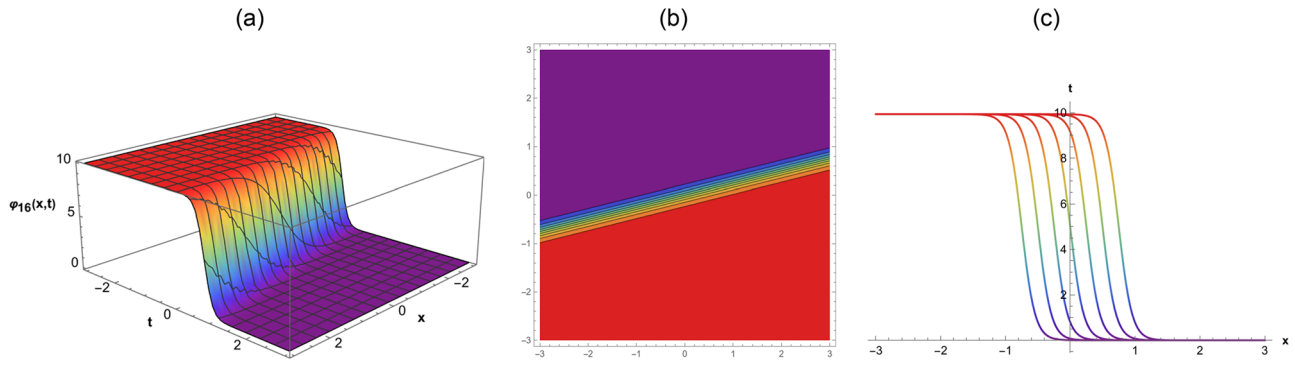

Figure 4: Kink soliton behavior of the solution $\varphi_{16}(x, t)$ for the parameter values $n = 0, m = -1, \nu = 1.5, \beta = 0.5, k = 0.2, F = 1.5$, and $D = 1$: (a) three-dimensional plot, (b) contour plot, and (c) two-dimensional plot.

- If $n = \chi$, $m = r$, $\chi(r \neq 0)$, and $\nu = 0$, then

$$\varphi_{32}(x, t) = \frac{1}{k^2}(Dkn \ln(F) - Dk\sqrt{\sigma} \ln(F)) + \frac{1}{k}\{2D\nu \ln(F)(F^{\ddot{\varrho}\chi} - r)\}. \tag{86}$$

- When $n = \nu = 0$, then

$$\varphi_{33}(x, t) = \frac{1}{k^2}(Dkn \ln(F) - Dk\sqrt{\sigma} \ln(F)) + \frac{1}{k}(2D\zeta m\nu \ln^2(F)). \tag{87}$$

- When $n = m = 0$, then

$$\varphi_{34}(x, t) = \frac{1}{k^2}(Dkn \ln(F) - Dk\sqrt{\sigma} \ln(F)) - \frac{2D}{\zeta k}. \tag{88}$$

- When $m = 0$ and $n \neq 0$, then

$$\varphi_{35}(x, t) = \frac{Dkn \ln(F) - Dk\sqrt{\sigma} \ln(F)}{k^2} - \frac{2Dnp \ln(F)}{k(\cosh_F(\zeta n) - \sinh_F(\zeta n) + p)}, \tag{89}$$

$$\varphi_{36}(x, t) = \frac{Dkn \ln(F) - Dk\sqrt{\sigma} \ln(F)}{k^2} - \frac{2Dn \ln(F)(\cosh_F(\zeta n) + \sinh_F(\zeta n))}{k(\cosh_F(\zeta n) + \sinh_F(\zeta n) + q)}. \tag{90}$$

- When $n = \chi, \nu = r\chi(r \neq 0)$, and $m = 0$, then

$$\varphi_{37}(x, t) = \frac{Dkn \ln(F) - Dk\sqrt{\sigma} \ln(F)}{k^2} - \frac{2D\nu \ln(F) pF^{\ddot{\varrho}\chi}}{k(p - rqF^{\ddot{\varrho}\chi})}. \tag{91}$$

3.2 Quartic model

By applying the traveling wave transformation, we readily obtain the nonlinear ODE

$$D\psi'' + w\psi' - k\psi\psi' + \alpha\psi - \beta\psi^4 = 0. \tag{92}$$

Observe that we obtain that $N = 1$ by using the balance between the dispersive and nonlinear terms in Eq. (92). Therefore, the solutions of this equation are expected to be expressed in similar fashion as for Eq. (50). By substituting Eq. (50) together with its derivatives into Eq. (92) and by comparing the coefficients of the indices of $\Omega(\zeta)$, we can obtain an algebraic system of equations. The solutions lead to two possible families of parameters

Family 1.

$$b_0 = -\frac{\sqrt{\beta^2k^2 \ln^2 F(n^2 - 4m\nu)} + \beta kn \ln(F)}{2\beta^2}, \tag{93}$$

$$b_1 = -\frac{k\nu \ln(F)}{\beta}, \tag{94}$$

$$w = -\frac{3k^3 \ln^2 F(n^2 - 4m\nu)}{2\beta^2}, \tag{95}$$

$$D = -\frac{k^2\sqrt{\beta^2k^2 \ln^2 F(n^2 - 4m\nu)}}{2\beta^3}, \tag{96}$$

$$\alpha = -\frac{(\beta^2k^2 \ln^2 F(n^2 - 4m\nu))^{3/2}}{\beta^5}. \tag{97}$$

Family 2.

$$b_0 = -\frac{\sqrt{3}\sqrt{\beta^2(-k^2) \ln^2 F(n^2 - 4m\nu)} + 3\beta kn \ln(F)}{6\beta^2}, \tag{98}$$

$$b_1 = -\frac{k\nu \ln(F)}{\beta}, \tag{99}$$

$$w = \frac{k^3 \ln^2 F(n^2 - 4m\nu)}{6\beta^2}, \tag{100}$$

$$D = -\frac{k^2\sqrt{\beta^2(-k^2) \ln^2 F(n^2 - 4m\nu)}}{2\sqrt{3}\beta^3}, \tag{101}$$

$$\alpha = \frac{(\beta^2(-k^2)\ln^2 F(n^2 - 4m\nu))^{3/2}}{3\sqrt{3}\beta^5}. \tag{102}$$

Proceeding as in the case of the model with quadratic reaction law, we obtain the following traveling wave solutions for Eq. (2).

• When $n^2 - 4m\nu < 0$ and $\nu \neq 0$, then

$$\varphi_1(x,t) = -\frac{1}{2\beta^2}(\sqrt{\beta^2k^2\sigma\ln^2 F} + \beta kn\ln F) - \frac{1}{\beta}\left\{k\nu\ln F\left(\frac{\sqrt{-\sigma}\tan_F\left(\frac{\zeta\sqrt{-\sigma}}{2}\right)}{2\nu} - \frac{n}{2\nu}\right)\right\}, \tag{103}$$

$$\varphi_2(x,t) = -\frac{1}{2\beta^2}(\sqrt{\beta^2k^2\sigma\ln^2 F} + \beta kn\ln F) - \frac{1}{\beta}\left\{k\nu\ln F\left(-\frac{\sqrt{-\sigma}\cot_F\left(\frac{\zeta\sqrt{-\sigma}}{2}\right)}{2\nu} - \frac{n}{2\nu}\right)\right\}, \tag{104}$$

$$\varphi_3(x,t) = -\frac{1}{2\beta^2}(\sqrt{\beta^2k^2\sigma\ln^2 F} + \beta kn\ln(F)) - \frac{1}{\beta}\left\{k\nu\ln(F)\left(\frac{\sqrt{-\sigma}(\tan_F(\zeta\sqrt{-\sigma}) - \sec_F(\zeta\sqrt{-\sigma}))}{2\nu} - \frac{n}{2\nu}\right)\right\}, \tag{105}$$

$$\varphi_4(x,t) = -\frac{1}{2\beta^2}(\sqrt{\beta^2k^2\sigma\ln^2 F} + \beta kn\ln(F)) - \frac{1}{\beta}\left\{k\nu\ln(F)\left(-\frac{\sqrt{-\sigma}(\cot_F(\zeta\sqrt{-\sigma}) - \sqrt{pq}\csc_F(\zeta\sqrt{-\sigma}))}{2\nu} - \frac{n}{2\nu}\right)\right\}, \tag{106}$$

$$\varphi_5(x,t) = -\frac{1}{2\beta^2}(\sqrt{\beta^2k^2\sigma\ln^2 F} + \beta kn\ln(F)) - \frac{1}{\beta}\left\{k\nu\ln(F)\left(\frac{\sqrt{-\sigma}\left(\tan_F\left(\frac{\zeta\sqrt{-\sigma}}{4}\right) - \cot_F\left(\frac{\zeta\sqrt{-\sigma}}{4}\right)\right)}{4\nu} - \frac{n}{2\nu}\right)\right\}. \tag{107}$$

For the sake of convenience, Figure 5 shows graphs of the solution $\varphi_1(x,t)$ for the parameter values $n = 1$, $m = 1$, $\nu = 1.5$, $\beta = 1$, $k = 1.2$, and $F = 1.5$.

• When $n^2 - 4m\nu > 0$ and $\nu \neq 0$, then

$$\varphi_6(x,t) = -\frac{1}{2\beta^2}(\sqrt{\beta^2k^2\sigma\ln^2 F} + \beta kn\ln F) - \frac{1}{\beta}\left\{k\nu\ln F\left(-\frac{n}{2\nu} - \frac{\sqrt{\sigma}\tanh_F\left(\frac{\zeta\sqrt{\sigma}}{2}\right)}{2\nu}\right)\right\}, \tag{108}$$

$$\varphi_7(x,t) = -\frac{1}{2\beta^2}(\sqrt{\beta^2k^2\sigma\ln^2 F} + \beta kn\ln F) - \frac{1}{\beta}\left\{k\nu\ln F\left(-\frac{\sqrt{\sigma}\coth_F\left(\frac{\zeta\sqrt{\sigma}}{2}\right)}{2\nu} - \frac{n}{2\nu}\right)\right\}, \tag{109}$$

$$\varphi_8(x,t) = -\frac{1}{2\beta^2}(\sqrt{\beta^2k^2\sigma\ln^2 F} + \beta knLn(F)) - \frac{1}{\beta}\left\{k\nu\ln(F)\left(-\frac{n}{2\nu} - \frac{\sqrt{\sigma}(\tanh_F(\zeta\sqrt{\sigma}) \pm i\sqrt{pq}\,\mathrm{sech}_F(\zeta\sqrt{\sigma}))}{2\nu}\right)\right\}, \tag{110}$$

$$\varphi_9(x,t) = -\frac{1}{2\beta^2}(\sqrt{\beta^2k^2\sigma\ln^2 F} + \beta kn\ln(F)) - \frac{1}{\beta}\left\{k\nu\ln(F)\left(-\frac{\sqrt{\sigma}(\coth_F(\zeta\sqrt{\sigma}) \pm \sqrt{pq}\,\mathrm{csch}_F(\zeta\sqrt{\sigma}))}{2\nu} - \frac{n}{2\nu}\right)\right\}, \tag{111}$$

$$\varphi_{10}(x,t) = -\frac{1}{2\beta^2}(\sqrt{\beta^2k^2\sigma\ln^2 F} + \beta kn\ln(F)) - \frac{1}{\beta}\left\{k\nu\ln(F)\left(-\frac{\sqrt{\sigma}\left(\coth_F\left(\frac{\zeta\sqrt{\sigma}}{4}\right) + \tanh_F\left(\frac{\zeta\sqrt{\sigma}}{4}\right)\right)}{4\nu} - \frac{n}{2\nu}\right)\right\}. \tag{112}$$

For illustration purposes, Figure 6 shows the graphical behavior of the solution $\varphi_6(x,t)$ for the parameter values $n = 1$, $m = 2$, $\nu = -1.5$, $\beta = 1$, $k = 1.7$, and $F = 1.5$.

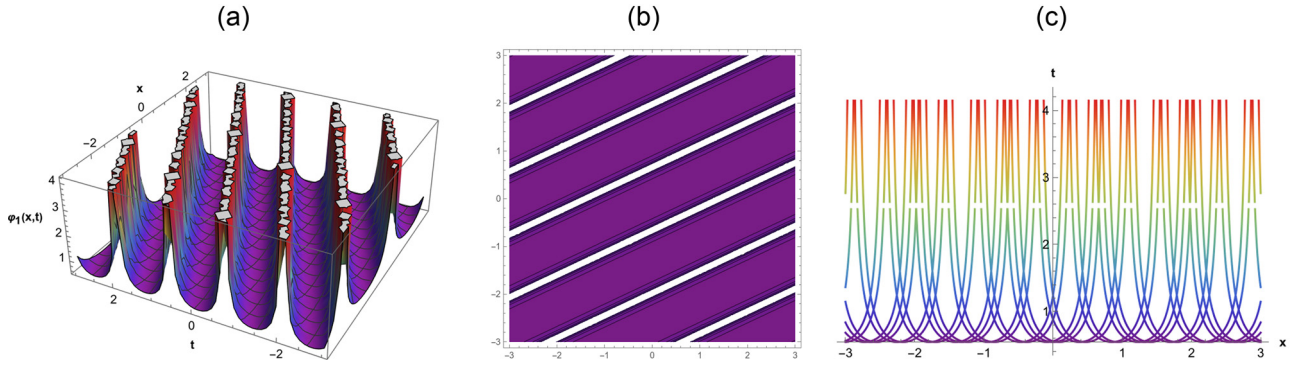

Figure 5: Solitary wave behavior of the solution $\varphi_1(x, t)$ for the parameter values $n = 1$, $m = 1$, $\nu = 1.5$, $\beta = 1$, $k = 1.2$, and $F = 1.5$: (a) three-dimensional plot, (b) contour plot, and (c) two-dimensional plot.

- If $m\nu > 0$ and $n = 0$, then

$$\varphi_{11}(x,t) = -\frac{1}{2\beta^2}\left(\sqrt{\beta^2k^2\sigma \ln^2 F} + \beta kn \ln(F)\right) - \frac{1}{\beta}\left[k\nu \ln(F)\sqrt{\frac{m}{\nu}} \tan_F(\zeta\sqrt{m\nu})\right], \tag{113}$$

$$\varphi_{12}(x,t) = \frac{1}{\beta}\left[k\nu \ln(F)\sqrt{\frac{m}{\nu}} \cot_F(\zeta\sqrt{m\nu})\right] - \frac{1}{2\beta^2}\left(\sqrt{\beta^2k^2\sigma \log^2 F} + \beta kn \ln(F)\right), \tag{114}$$

$$\varphi_{13}(x,t) = -\frac{1}{2\beta^2}\left(\sqrt{\beta^2k^2\sigma \ln^2 F} + \beta kn \ln(F)\right) - \frac{1}{\beta}\left[k\nu \ln(F)\sqrt{\frac{m}{\nu}} (\tan(2\zeta\sqrt{m\nu}) \pm \sqrt{pq}\, \sec_F(2\zeta\sqrt{m\nu}))\right], \tag{115}$$

$$\varphi_{14}(x,t) = -\frac{1}{2\beta^2}\left(\sqrt{\beta^2k^2\sigma \ln^2 F} + \beta kn \ln(F)\right) + \frac{1}{\beta}\left[k\nu \ln(F)\sqrt{\frac{m}{\nu}} (\cot_F(2\zeta\sqrt{m\nu}) \pm \sqrt{pq}\, \csc_F(2\zeta\sqrt{m\nu}))\right], \tag{116}$$

$$\varphi_{15}(x,t) = -\frac{1}{2\beta^2}\left(\sqrt{\beta^2k^2\sigma \ln^2 F} + \beta kn \ln(F)\right) - \frac{1}{2\beta}\left[k\nu \ln(F)\sqrt{\frac{m}{\nu}}\left(\tan_F\left(\frac{1}{2}\zeta\sqrt{m\nu}\right) - \cot_F\left(\frac{1}{2}\zeta\sqrt{m\nu}\right)\right)\right]. \tag{117}$$

- When $m\nu < 0$ and $n = 0$, then

$$\varphi_{16}(x,t) = -\frac{1}{2\beta^2}\left(\sqrt{\beta^2k^2\sigma \ln^2 F} + \beta kn \ln(F)\right) + \frac{1}{\beta}\left[k\nu \ln(F)\sqrt{-\frac{m}{\nu}} \tanh_F(\zeta\sqrt{-m\nu})\right], \tag{118}$$

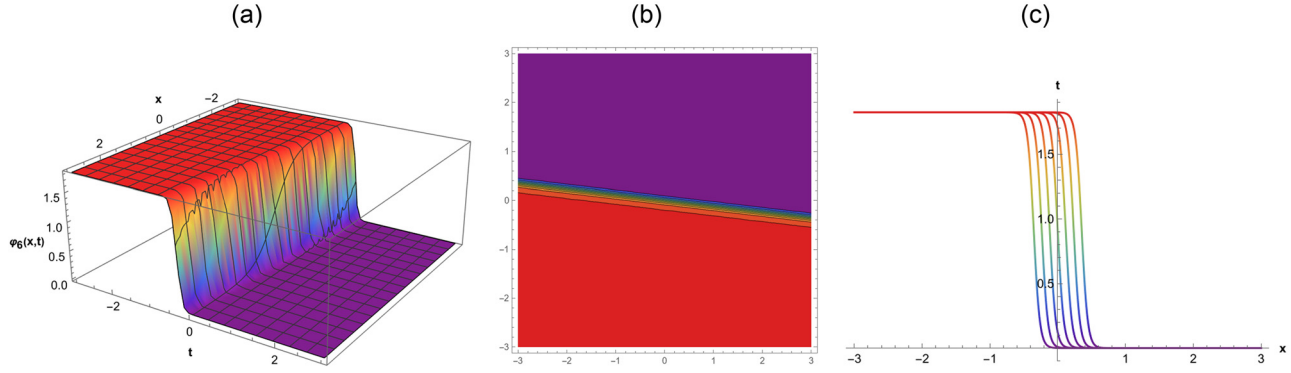

Figure 6: Kink soliton behavior of the solution $\varphi_6(x, t)$ for the parameter values $n = 1, m = 2, \nu = 1.5, \beta = 1, k = 1.7$, and $F = 1.5$: (a) three-dimensional plot, (b) contour plot, and (c) two-dimensional plot.

$$\varphi_{17}(x,t) = -\frac{1}{2\beta^2}\left(\sqrt{\beta^2k^2\sigma\ln^2 F} + \beta kn\ln(F)\right) + \frac{1}{\beta}\left\{k\nu\ln(F)\sqrt{-\frac{m}{\nu}}\coth_F\left(\zeta\sqrt{-m\nu}\right)\right\}, \tag{119}$$

$$\varphi_{18}(x,t) = -\frac{1}{2\beta^2}\left(\sqrt{\beta^2k^2\sigma\ln^2 F} + \beta kn\ln(F)\right) + \frac{1}{\beta}\left\{k\nu\ln(F)\sqrt{-\frac{m}{\nu}}\left(\tanh_F(2\zeta\sqrt{-m\nu}) + i\sqrt{pq}\,\mathrm{sech}_F(2\zeta\sqrt{-m\nu})\right)\right\}, \tag{120}$$

$$\varphi_{19}(x,t) = -\frac{1}{2\beta^2}\left(\sqrt{\beta^2k^2\sigma\ln^2 F} + \beta kn\ln(F)\right) + \frac{1}{\beta}\left\{k\nu\ln(F)\sqrt{-\frac{m}{\nu}}\left(\coth_F(2\sqrt{-m\nu}) \pm \sqrt{pq}\,\mathrm{csch}_F(2\sqrt{-m\nu})\right)\right\}, \tag{121}$$

$$\varphi_{20}(x,t) = -\frac{1}{2\beta^2}\left(\sqrt{\beta^2k^2\sigma\ln^2 F} + \beta kn\ln(F)\right) + \frac{1}{2\beta}\left\{k\nu\ln(F)\sqrt{-\frac{m}{\nu}}\left(\tanh_F\left(\frac{1}{2}\zeta\sqrt{-m\nu}\right) - \coth_F\left(\frac{1}{2}\zeta\sqrt{-m\nu}\right)\right)\right\}. \tag{122}$$

Figure 7 shows the solution $\varphi_{16}(x,t)$ for the parameter values $n = 0$, $m = 1$, $\nu = -1.5$, $\beta = 1.5$, $k = 1.5$, and $F = 1.5$.

- If $n = 0$ and $m = \nu$, then

$$\varphi_{21}(x,t) = -\frac{1}{2\beta^2}\left(\sqrt{\beta^2k^2\sigma\ln^2 F} + \beta kn\ln(F)\right) - \frac{1}{\beta}(k\nu\ln(F)\tan_F(\zeta m)), \tag{123}$$

$$\varphi_{22}(x,t) = -\frac{1}{2\beta^2}\left(\sqrt{\beta^2k^2\sigma\mathrm{Ln}F^2} + \beta kn\ln(F)\right) + \frac{1}{\beta}(k\nu\ln(F)\cot_F(\zeta m)), \tag{124}$$

$$\varphi_{23}(x,t) = -\frac{1}{2\beta^2}\left(\sqrt{\beta^2k^2\sigma\ln^2 F} + \beta kn\ln(F)\right) - \frac{1}{\beta}\{k\nu\ln(F)(\tan_F(2\zeta m) \pm \sqrt{pq}\sec_F(2\zeta m))\}, \tag{125}$$

$$\varphi_{24}(x,t) = -\frac{1}{2\beta^2}\left(\sqrt{\beta^2k^2\sigma\ln^2 F} + \beta kn\ln(F)\right) - \frac{1}{\beta}\{k\nu\ln(F)(-\cot_F(2\zeta m) \pm \sqrt{pq}\csc_F(2\zeta m))\}, \tag{126}$$

$$\varphi_{25}(x,t) = -\frac{1}{2\beta^2}\left(\sqrt{\beta^2k^2\sigma\ln^2 F} + \beta kn\ln(F)\right) - \frac{1}{2\beta}\left\{k\nu\ln(F)\left(\tan_F\left(\frac{\zeta m}{2}\right) - \cot_F\left(\frac{\zeta m}{2}\right)\right)\right\}. \tag{127}$$

Figure 8 shows the graphical behavior of the solution $\varphi_{21}(x,t)$ for the parameter values $n = 0$, $m = 1.5$, $\nu = 1.5$, $\beta = 1.5$, $k = 1.1$, and $F = 1.5$.

- When $n = 0$ and $\nu = -m$, then

$$\varphi_{26}(x,t) = -\frac{1}{2\beta^2}\left(\sqrt{\beta^2k^2\,\sigma\mathrm{Ln}F^2} + \beta kn\ln(F)\right) + \frac{1}{\beta}(k\nu\ln(F)\tanh_F(\zeta m)), \tag{128}$$

$$\varphi_{27}(x,t) = -\frac{1}{2\beta^2}\left(\sqrt{\beta^2k^2\sigma\ln^2 F} + \beta kn\ln(F)\right) + \frac{1}{\beta}(k\nu\ln(F)\coth_F(\zeta m)), \tag{129}$$

$$\varphi_{28}(x,t) = -\frac{1}{2\beta^2}\left(\sqrt{\beta^2k^2\sigma\ln^2 F} + \beta kn\ln(F)\right) - \frac{1}{\beta}\{k\nu\ln(F)(-\tanh_F(2\zeta m) + i\sqrt{pq}\,\mathrm{sech}_F(2\zeta m))\}, \tag{130}$$

$$\varphi_{29}(x,t) = -\frac{1}{2\beta^2}\left(\sqrt{\beta^2k^2\sigma\ln^2 F} + \beta kn\ln(F)\right) - \frac{1}{\beta}\{k\nu\ln(F)(\sqrt{pq}\,\mathrm{csch}_F(2\zeta m) - \coth_F(2\zeta m))\}, \tag{131}$$

$$\varphi_{30}(x,t) = -\frac{1}{2\beta^2}\left(\sqrt{\beta^2k^2\sigma\ln^2 F} + \beta kn\ln(F)\right) - \frac{1}{2\beta}\left\{k\nu\ln(F)\left(-\coth_F\left(\frac{\zeta m}{2}\right) - \tanh_F\left(\frac{\zeta m}{2}\right)\right)\right\}. \tag{132}$$

- If $n^2 = 4m\nu$, then

$$\varphi_{31}(x,t) = -\frac{1}{2\beta^2}\left(\sqrt{\beta^2k^2\sigma\ln^2 F} + \beta kn\ln(F)\right) + \frac{1}{\beta\zeta n^2}\{2km\nu(\zeta n\ln(F) + 2)\}. \tag{133}$$

- When $n = \chi$, $m = r\chi$ with $r \neq 0$ and $\nu = 0$, then

$$\varphi_{32}(x,t) = -\frac{1}{2\beta^2}\left(\sqrt{\beta^2k^2\sigma\ln^2 F} + \beta kn\ln(F)\right) - \frac{1}{\beta}\{k\nu\ln(F)(F^{\zeta\chi} - r)\}. \tag{134}$$

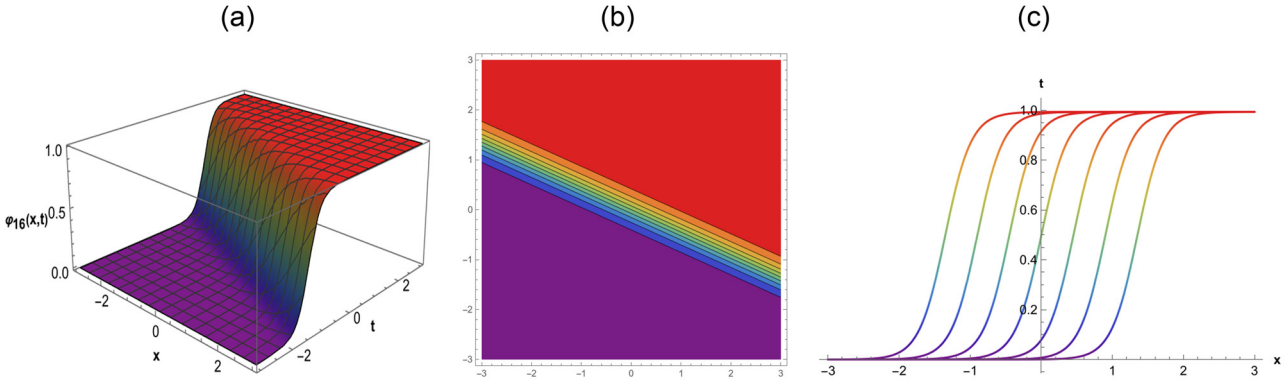

Figure 7: Anti-Kink soliton behavior of the solution $\varphi_{16}(x, t)$ for the parameter values $n = 0$, $m = 1$, $\nu = 1.5$, $\beta = 1.5$, $k = 1.5$, and $F = 1.5$: (a) three-dimensional plot, (b) contour plot, and (c) two-dimensional plot.

- When $n = \nu = 0$ then

$$\varphi_{33}(x, t) = -\frac{1}{2\beta^2}\left(\sqrt{\beta^2 k^2 \sigma \ln^2 F} + \beta k n \ln(F)\right) - \frac{1}{\beta}(\zeta k m \nu \ln^2 F). \tag{135}$$

- If $n = m = 0$, then

$$\varphi_{34}(x, t) = -\frac{1}{2\beta^2}\left(\sqrt{\beta^2 k^2 \sigma \ln^2 F} + \beta k n \ln(F)\right) + \frac{k}{\beta\zeta}. \tag{136}$$

- When $=m = 0$ and $\nu \neq 0$, then

$$\varphi_{35}(x, t) = -\frac{\sqrt{\beta^2 k^2 \sigma \ln^2 F} + \beta k n \ln(F)}{2\beta^2} + \frac{k n p \ln(F)}{\beta(\cosh_F(\zeta n) - \sinh_F(\zeta n) + p)}, \tag{137}$$

$$\varphi_{36}(x, t) = -\frac{\beta k \sqrt{\sigma} \ln(F) + \beta k n \ln(F)}{2\beta^2} + \frac{k n \ln(F)(\cosh_F(\zeta n) + \sinh_F(\zeta n))}{\beta(\cosh_F(\zeta n) + \sinh_F(\zeta n) + q)}. \tag{138}$$

- If $n = \chi$, $\nu = r\chi$ with $r \neq 0$, and $m = 0$, then

$$\varphi_{37}(x, t) = \frac{k\nu p \ln(F) F^{\zeta\chi}}{\beta(p - qrF^{\zeta\chi})} - \frac{\beta k n \ln(F) + \sqrt{\sigma}}{2\beta^2}. \tag{139}$$

4 Discussion

In this section, we will discuss the graphical representation of the results obtained in the previous section by using the new NEDAM. Different types of soliton solutions are seen, including solitary wave, kink, anti-kink, and rational function solutions. Using the Mathematica 11.1 software, graphs have been created to show the solutions physical behavior in the form of 3D, 2D and contour plots. When modeling a variety of physical phenomena (such as chemical reactions, the creation of biological patterns, and heat conduction), reaction–diffusion equations with quadratic and quartic nonlinearities may essential.

It is well known that solitary waves are examples of coherent structures that propagate without distortion because of their limited and stable profiles. The study of

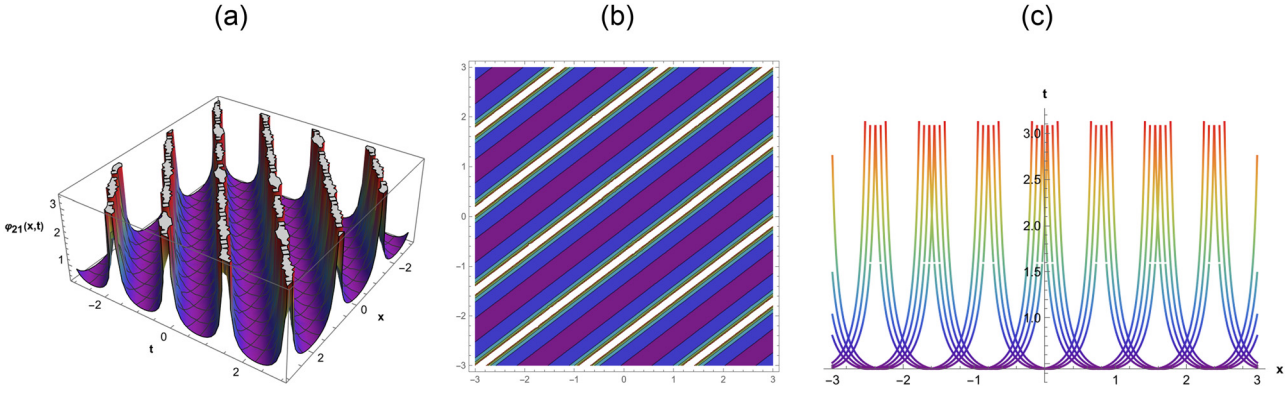

Figure 8: Solitary wave behavior of the solution $\varphi_{21}(x, t)$ for the parameter values $n = 0$, $m = 1.5$, $\nu = 1.5$, $\beta = 1.5$, $k = 1.1$, and $F = 1.5$: (a) three-dimensional plot, (b) contour plot, and (c) two-dimensional plot.

energy transfer mechanisms in nonlinear media, including shallow water systems and optical fibers, depends heavily on these waves. Kink and anti-kink solutions, which are frequently used to mimic interfaces or domain walls like those seen in magnetic phase transitions or crystal dislocations, represent monotonic transitions between two stable states. Understanding phase separation and symmetry-breaking dynamics in physical systems requires an understanding of these structures. Less frequently found, rational function solutions describe limited structures with distinctive singular behaviors. These are frequently linked to severe occurrences or anomaly-driven phenomena, such as localized bursts in reaction–diffusion systems or rogue waves in hydrodynamics. Many waveforms and transition patterns are possible due to the interaction between the quadratic and quartic nonlinearities in these equations, which enriches the solution space. Visualizing these solutions offers important information about their stability, dynamics over time and space, and possible uses in systems controlled by complicated pattern generation, phase transitions, and nonlinear energy transfer. In particular, Figure 1 depicts a lump-kink, while Figures 2, 4, and 6 are kink solitons. Figures 3, 5, and 8 provide solitary waves, and Figure 7 shows an anti-kink behavior.

5 Conclusions

In this work, the NEDAM has been used to obtain solitary wave solutions for general reaction–diffusion equations with quadratic and quartic nonlinearities. By applying this approach, we have established different types of soliton solutions, including solitary wave, kink, anti-kink, and rational function solutions. To illustrate the physical behavior of the solutions, some plots have been obtained using the Mathematica software. One can obtain various possible results by adjusting the parametric values appropriately. As a conclusion on the side, we have found out that the NEDAM is an appropriate and reliable method for locating precise soliton solutions for broad categories of nonlinear problems. The results obtained in this work were verified by substituting them into the original model equations with the help of Mathematica software. We verified in all cases that the functions derived in this work are actually solutions of our mathematical models. As a future direction of investigation, the models investigated in this work will be extended as NPDEs of higher-order partial differential equations, considering fractional orders of differentiation, and stochastic sources. In those cases, we expect to derive solitary wave solutions by employing the NEDAM, and we will confirm our result numerically through suitable mathematical software.

Acknowledgments: The authors wish to thank the anonymous reviewers for their criticisms. All of their suggestions contributed to improving the quality of this work.

Funding information: One of the authors of this work (J.E.M.-D.) wishes to acknowledge the financial support from the National Council of Humanities, Science and Technology of Mexico (CONACYT) through grant A1-S-45928, associated to the research project “Conservative methods for fractional hyperbolic systems: analysis and applications.” In turn, M.G.M.-G. acknowledges the financial support from the program PROSNI of the University of Guadalajara, Mexico.

Author contributions: Conceptualization: N.A., J.E.M.-D., M.A., M.J., M.Z.B., M.G.M.-G.; data curation: N.A., J.E.M.-D., M.A., M.J., M.Z.B., M.G.M.-G.; formal analysis: N.A., J.E.M.-D., M.A., M.J., M.Z.B.; funding acquisition: J.E.M.-D., M.G.M.-G.; investigation: N.A., J.E.M.-D., M.A., M.J., M.Z.B., M.G.M.-G.; methodology: N.A., J.E.M.-D., M.A., M.J., M.Z.B., M.G.M.-G.; project administration: J.E.M.-D., M.G.M.-G.; resources: J.E.M.-D., M.G.M.-G.; software: N.A., J.E.M.-D., M.A., M.J., M.Z.B., M.G.M.-G.; supervision: N.A., J.E.M.-D.; validation: N.A., J.E.M.-D., M.A., M.J., M.Z.B., M.G.M.-G.; visualization: N.A., J.E.M.-D., M.A., M.J., M.Z.B., M.G.M.-G.; roles/writing – original draft: N.A., J.E.M.-D., M.A., M.J., M.Z.B., M.G.M.-G.; writing – review editing: N.A., J.E.M.-D., M.A., M.J., M.Z.B., M.G.M.-G. All authors have accepted responsibility for the entire content of this manuscript and approved its submission.

Conflict of interest: The authors state no conflict of interest.

Data availability statement: All data generated or analysed during this study are included in this published article.

References

[1] Az-Zobi EA, Alomari QM, Afef K, Inc M. Dynamics of generalized time-fractional viscous-capillarity compressible fluid model. Opt Quantum Electron. 2024;56(4):629.

[2] Fakih H, Faour M, Saoud W, Awad Y. On the complex version of the Cahn-Hilliard-Oono type equation for long interactions phase separation. Int J Math Comput Eng. 2024;2(2):233–59.

[3] Inc M, Az-Zobi EA, Jhangeer A, Rezazadeh H, Nasir Ali M, Kaabar MK. New soliton solutions for the higher-dimensional non-local Ito equation. Nonlinear Eng. 2021;10(1):374–84.

[4] Az-Zo’bi EA, Al Dawoud K, Marashdeh M. Numeric-analytic solutions of mixed-type systems of balance laws. Appl Math Comput. 2015;265:133–43.

[5] Rahman RU, Al-Maaitah AF, Qousini M, Az-Zobi EA, Eldin SM, Abuzar M. New soliton solutions and modulation instability analysis of fractional Huxley equation. Results Phys. 2023;44:106163.
[6] Az-Zobi E, Akinyemi L, Alleddawi AO. Construction of optical solitons for conformable generalized model in nonlinear media. Modern Phys Lett B. 2021;35(24):2150409.
[7] El-Sherif AA, Shoukry MM. Coordination properties of tridentate (N, O, O) heterocyclic alcohol (PDC) with Cu (II): Mixed ligand complex formation reactions of Cu (II) with PDC and some bio-relevant ligands. Spectrochimica Acta Part A Mol Biomol Spectroscopy. 2007;66(3):691–700.
[8] Malik S, Almusawa H, Kumar S, Wazwaz AM, Osman MSA. (2+1)-dimensional Kadomtsev-Petviashvili equation with competing dispersion effect: Painlevé analysis, dynamical behavior and invariant solutions. Results Phys. 2021;23:104043.
[9] Shakeel M, Liu X, Mostafa AM, AlQahtani SA, AlQahtani NF, Ali MR. Exploring of soliton solutions in optical metamaterials with parabolic law of nonlinearity. Opt Quantum Electronics. 2024;56(5):860.
[10] Shakeel M, Liu X, Mostafa AM, AlQahtani NF, Alameri A. Dynamic Solitary Wave Solutions Arising in Nonlinear Chains of Atoms Model. J Nonl Math Phys. 2024;31(1):70.
[11] Abdeljabbar A, Roshid HO, Aldurayhim A. Bright, dark, and rogue wave soliton solutions of the quadratic nonlinear Klein-Gordon equation. Symmetry. 2022;14(6):1223.
[12] Wang M, Zhou Y, Li Z. Application of a homogeneous balance method to exact solutions of nonlinear equations in mathematical physics. Phys Lett A. 1996;216(1–5):67–75.
[13] Radha B and Duraisamy C. Retracted article: The homogeneous balance method and its applications for finding the exact solutions for nonlinear equations. J Ambient Intel Humanized Comput. 2021;12(6):6591–7.
[14] Kumar D, Park C, Tamanna N, Paul GC, Osman MS. Dynamics of two-mode Sawada-Kotera equation: Mathematical and graphical analysis of its dual-wave solutions. Results Phys. 2020;19:103581.
[15] Rahman MM, Habib MA, Ali HS, Miah MM. The generalized Kudryashov method: a renewed mechanism for performing exact solitary wave solutions of some NLEEs. J Mech Cont Math. 2019;14(1):323–39.
[16] Jabbari A, Kheiri H. New exact traveling wave solutions for the Kawahara and modified Kawahara equations by using modified tanh–coth method. Acta Universitatis Apulensis. 2010;23:21–38.
[17] Bekir A, Cevikel AC. The tanh–coth method combined with the Riccati equation for solving nonlinear coupled equation in mathematical physics. J King Saud Univ-Sci. 2011;23(2):127–32.
[18] Seadawy AR, Alsaedi BA. Dynamical stricture of optical soliton solutions and variational principle of nonlinear Schrödinger equation with Kerr law nonlinearity. Modern Phys Lett B. 2024;38:2450254.
[19] Seadawy AR, Alsaedi BA. Variational principle and optical soliton solutions for some types of nonlinear Schrödinger dynamical systems. Int J Geometric Meth Modern Phys. 2024;21(6):2430004–245.
[20] Seadawy AR, Alsaedi BA. Variational principle for generalized unstable and modify unstable nonlinear Schrödinger dynamical equations and their optical soliton solutions. Opt Quantum Electronics. 2024;56(5):844.
[21] Zhang RF, Bilige S. Bilinear neural network method to obtain the exact analytical solutions of nonlinear partial differential equations and its application to p-gBKP equation. Nonl Dyn. 2019;95:3041–8.
[22] Rahman RU, Hammouch Z, Alsubaie ASA, Mahmoud KH, Alshehri A, Az-Zobi EA, et al. Dynamical behavior of fractional nonlinear dispersive equation in Murnaghanas rod materials. Results Phys. 2024;56:107207.
[23] Almatrafi MB. Construction of closed form soliton solutions to the space-time fractional symmetric regularized long wave equation using two reliable methods. Fractals. 2023;31(10):2340160.
[24] Almatrafi MB. Solitary wave solutions to a fractional model using the improved modified extended tanh-function method. Fractal Fract. 2023;7(3):252.
[25] Almatrafi MB, Alharbi A. New soliton wave solutions to a nonlinear equation arising in plasma physics. CMES-Comput Model Eng Sci. 2023;137(1) 827–41.
[26] Alharbi AR, Almatrafi MB. Exact solitary wave and numerical solutions for geophysical KdV equation. J King Saud Univ-Sci. 2022;34(6):102087.
[27] Raza N, Osman MS, Abdel-Aty AH, Abdel-Khalek S, Besbes HR. Optical solitons of space-time fractional Fokas-Lenells equation with two versatile integration architectures. Adv Differ Equ. 2020;2020:1–15.
[28] Shakeel M, Bibi A, Chou D, Zafar A. Study of optical solitons for Kudryashovas Quintuple power-law with dual form of nonlinearity using two modified techniques. Optik. 2023;273:170364.
[29] Yan Z, Lou S. Soliton molecules in Sharma–Tasso–Olver–Burgers equation. Appl Math Lett. 2020;104:106271.
[30] Wu Q, Wang S, Yao M, Niu Y, Wang C. Nonlinear dynamics of three-layer microplates: simultaneous presence of the micro-scale and imperfect effects. Europ Phys J Plus. 2024;139(5):1–21.
[31] Wang Z, Parastesh F, Natiq H, Li J, Xi X, Mehrabbeik M. Synchronization patterns in a network of diffusively delay-coupled memristive Chialvo neuron map. Phys Lett A. 2024;514:129607.
[32] Dai Z, Wolfsberg A, Lu Z, Ritzi Jr. R. Representing aquifer architecture in macrodispersivity models with an analytical solution of the transition probability matrix. Geophys Res Lett. 2007;34(20):L20406.
[33] Kai Y, Yin Z. On the Gaussian traveling wave solution to a special kind of Schrödinger equation with logarithmic nonlinearity. Modern Phys Lett B. 2022;36(02):2150543.
[34] Zhu C, Idris SA, Abdalla MEM, Rezapour S, Shateyi S, Gunay B. Analytical study of nonlinear models using a modified Schrödingeras equation and logarithmic transformation. Results Phys. 2023;55:107183.
[35] Zhu C, Al-Dossari M, Rezapour S, Shateyi S, Gunay B. Analytical optical solutions to the nonlinear Zakharov system via logarithmic transformation. Results Phys. 2024;56:107298.
[36] Berkal M, Almatrafi MB. Bifurcation and stability of two-dimensional activator–inhibitor model with fractional-order derivative. Fractal Fract. 2023;7(5):344.
[37] Sweilam NH, Ahmed SM, Adel M. A simple numerical method for two-dimensional nonlinear fractional anomalous sub-diffusion equations. Math Meth Appl Sci. 2021;44(4):2914–33.
[38] Adel M. Numerical simulations for the variable order two-dimensional reaction sub-diffusion equation: Linear and Nonlinear. Fractals. 2022;30(01):2240019.
[39] Adel M, Elsaid M. An efficient approach for solving fractional variable order reaction sub-diffusion based on Hermite formula. Fractals. 2022;30(01):2240020.
[40] Adel M. Finite difference approach for variable order reaction-subdiffusion equations. Adv Differ Equ. 2018;2018(1):406.
[41] Triki H, Leblond H, Mihalache D. Soliton solutions of nonlinear diffusion–reaction-type equations with time-dependent coefficients accounting for long-range diffusion. Nonl Dyn. 2016;86:2115–26.

[42] Bhardwaj SB, Singh RM, Sharma K, Mishra SC. Periodic and solitary wave solutions of cubic-quintic nonlinear reaction-diffusion equation with variable convection coefficients. Pramana. 2016;86:1253–8.
[43] Malik A, Chand F, Kumar H, Mishra SC. Exact solutions of nonlinear diffusion–reaction equations. Indian J Phys. 2012;86(2):129–36.
[44] Malik A, Kumar H, Chahal RP, Chand F. A dynamical study of certain nonlinear diffusion–reaction equations with a nonlinear convective flux term. Pramana. 2019;92:1–13.
[45] Vahidi J, Zabihi A, Rezazadeh H, Ansari R. New extended direct algebraic method for the resonant nonlinear Schrödinger equation with Kerr law nonlinearity. Optik. 2021;227:165936.
[46] Mirhosseini-Alizamini SM, Rezazadeh H, Srinivasa K, Bekir A. New closed form solutions of the new coupled Konno-Oono equation using the new extended direct algebraic method. Pramana. 2020;94(1):52.
[47] Munawar M, Jhangeer A, Pervaiz A, Ibraheem F. New general extended direct algebraic approach for optical solitons of Biswas-Arshed equation through birefringent fibers. Optik. 2021;228:165790.
[48] Bilal M, Ren J, Alsubaie ASA, Mahmoud KH, Inc M. Dynamics of nonlinear diverse wave propagation to Improved Boussinesq model in weakly dispersive medium of shallow waters or ion acoustic waves using efficient technique. Opt Quantum Electron. 2024;56(1):21.